JOM Journal of Optical Microsystems

RESEARCH PAPER

Micro-transfer printing of thick optical components using a tether-free UV-curable approach

Saif Wakeel,[a,*] Padraic E. Morrisey,[a] Muhammet Genc,[b] Prasanna Ramaswamy,[c] Robert Bernson,[a] Kamil Gradkowski,[a] Brian Corbett,[b] and Peter O'Brien[a]

[a]University College Cork, Tyndall National Institute, Photonics Packaging Group, Cork, Ireland
[b]University College Cork, Tyndall National Institute, Photonics Group, Cork, Ireland
[c]X-Celeprint Ltd., Cork, Ireland

ABSTRACT. Micro-transfer printing (μTP) has been widely used to integrate photonic components, such as lasers, modulators, photodetectors, micro-LEDs, on Si photonic platforms. There is a push toward the μTP of optical components in photonics packaging as it enables wafer-scale integration with high alignment accuracy. We demonstrate for the first time the μTP of thick optical components, such as micro-lenses, in the range of 250 to 1000 μm thickness. We explore the reliability of bonding such components using an ultraviolet (UV) curable epoxy and compare them with the current state of the art. The results show that the average shear strength of lenses bonded with InterVia is 19 MPa which is higher than currently used optical epoxies. Also, μTP process has no effect on the surface roughness and microstructure of lenses. Using our approach, we demonstrate how thick silicon and fused silica lenses can be integrated into photonic integrated circuits (PICs) using a tether-free process that is highly scalable and robust.

 [DOI: 10.1117/1.JOM.4.1.011003]

Keywords: micro-transfer printing; micro-optics; micro-lenses; wafer-level photonic packaging; photonic integrated circuit packaging; bonding materials in packaging

Paper 23027SS received Sep. 1, 2023; revised Nov. 8, 2023; accepted Nov. 17, 2023; published Nov. 29, 2023.

1 Introduction

Micro-transfer printing (μTP) is a widely used scalable wafer bonding approach in which multiple devices of different or same sizes can be mechanically picked up from a source wafer using elastomeric polydimethylsiloxane (PDMS) stamp and printed on the desired target wafer with an adhesive layer, such as benzocyclobutene (BCB) or InterVia photoelectric.[1] μTP is an alternative technology to existing flip-chip packaging and wafer-level bonding methods. The preference of using μTP over other existing bonding methods is due to its higher scalability, testing of devices on native wafers, high alignment accuracy, high yield, and reduced cycling time.[1,2] So far, photonics, electronics, and optical devices have been successfully printed for specific applications as listed in Table 1.

Table 1 highlights a few works done to show the type of devices printed so far. Printed photonics devices have vast applications, such as building transceivers for communications, sensors, and displays. Photonic packaging technologies and processes, as used in telecom, datatelecom, and medical applications, typically require optical coupling to/from photonic integrated circuits (PICs) to fiber. In a typical packaging approach, fiber is bonded/fixed to a PIC with epoxy which could also be called a fixed connection approach. However, in applications, such

*Address all correspondence to Saif Wakeel, saif.wakeel@tyndall.ie

Table 1 Micro-transfer printed devices and their applications.

μTP devices	References
Photodetectors	3, 4
Micro-LED	5–7
III-V lasers	2, 4, 8–16
Photodiodes	17
Modulators	18, 19
Micro-ring resonators	20, 21
Transistors	22–28
GC	29
GaN micro lenses	30, 31

as medical devices, fixed connection will no longer be efficient as there are some pluggable or removable connectors required. This pluggability can be achieved using micro-lenses. The lens expands the beam size and collimates it so that light can transmit in and out of PIC to a higher distance/better alignment tolerance.[32] This expansion and collimation can also create an air gap between PIC and fiber interfaces, which enables pluggable connections. Another advantage of this contactless connection is to avoid damaging the optical surface.[33] In the pluggable approach as demonstrated by our group previously,[32,33] micro-lenses are integrated on a PIC or fiber using epoxy (Fig. 1). This approach suffers from material issues, such as instability and low reliability, at high temperature of epoxy and process-related issues including low scalability, low manufacturability, and higher cycling time. These issues can be mitigated by developing a pluggable photonic package using μTP process.

Recently, μTP of GaN lenses was demonstrated by a photonics group at the University of Strathclyde,[30,31] these lenses were released using AlGaN release layer with tether support. The microstructure, aperture, mode field diameter, and optical performance of lenses were evaluated. Also, the integration of these lenses on a waveguide was presented. However, the thicknesses and radius of curvature of these lenses were 2 μm and 6 to 10 μm, respectively. Small lenses can limit the beam size and alignment tolerances. Therefore, due to mode mismatch higher coupling efficiency cannot be obtained.[30,34] The conventional way of μTP is using a release layer and underetching while the tether holds the device. However, this technique is expensive, and it can only

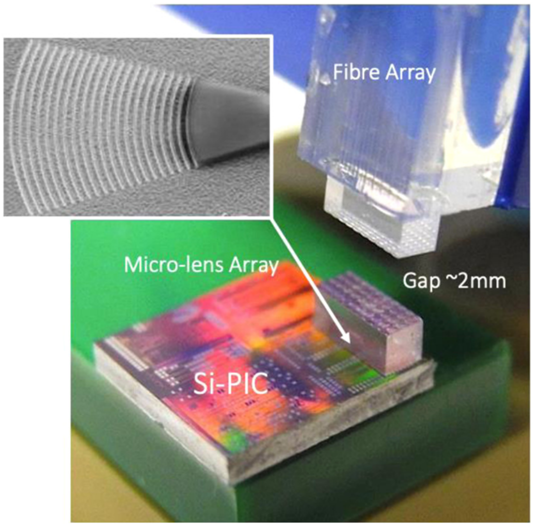

Fig. 1 Pluggable photonic packaging for bio-sensor applications.[30]

pick up and print a maximum of 20 to 30 μm thick coupons.[1,10,13,14,31,35] The work of the tether is to hold the entire footprint of coupons while the sacrifice layer is released. Tethers are generally made of resist, Si, SiN, etc., and these are defined by either spin coating or PECVD method. To make tethers for such thick devices (>250 μm), it is difficult to spin coat or deposit >250 μm thick resist, Si, and SiN. This suggests that large-footprint devices cannot be easily held and released from tether structures.

More recently, μTP of coupons with thicknesses up to 250 μm using a tether-less approach has been demonstrated by X-celeprint and Tyndall research groups. In the first work, coupons of thicknesses 15 to 250 μm were successfully picked up from UV dicing tape and printed on 3 μm InterVia coated silicon target wafers.[36] Printing yields of 100% and 63% to 66% were obtained for single stamp and array printing of 4 mm $\times$ 4.6 mm $\times$ 25 μm devices, respectively. No discussion about coupon sizes above 250 μm was made, also the effect of the pick-up and printing process on microstructure, surface roughness, and shear strength was not discussed or examined. In another work by a micro- and nanosystems group in Tyndall, μTP of 250 μm thick micro-inductors was described on a 2.2 μm thick InterVia coated silicon target wafer.[37] The statistical analysis of device performance (S-parameter) before and after printing was done. However, μTP of coupons with thicknesses >250 μm was not included and no study about the microstructure, roughness, and shear strength of printed coupons was performed for this either.

To the best of the authors' knowledge, μTP of thick optical components (250 to 1000 μm) has not been investigated to date and it presents an interesting approach to scalable photonics packaging where thick micro-lenses are used to enable pluggable or free space optical connections with relaxed alignment tolerances. The UV-release pick-up method for thick non-flat components has not been studied and the process effect of μTP on microstructure, shear strength, surface roughness, and alignment accuracy has not been examined. Therefore, the novelty of this study is to demonstrate μTP of 250 to 1000 μm thick optical lenses for the first time using the UV-release tether-less method. The microstructure, alignment accuracy, and surface roughness of thick lenses before and after printing are determined. Furthermore, a shear test of printed lenses before and after curing was performed and strength was compared with existing optical epoxies. The UV-release method allows the pick-up of thick devices and also has advantages in terms of being an etching-free and tether-free method, thereby reducing the overall cost of μTP utilization.

2 Experimental Procedures

This study demonstrates the proof of concept for μTP of thick optical components using the UV-release tether-less method. First, 500 μm thick silicon (Si) and fused-silica (FS) wafers are diced on UV-curable dicing tape with the same dimension as a 1×4 array of Si and 1×8 array of FS micro-lenses.[38,39] These diced pieces are named "pseudo lenses." The shear test of the pseudo lenses is performed using a Royce shear tester model 552 and compared with existing optical epoxies. Cross-section images of the bonded sample with InterVia and epoxy were obtained from a FEI Quanta 650 scanning electron microscope (SEM). To further demonstrate the possibility for μTP of actual lenses, a 380 μm thick off-the-shelf micro-lens array (part no. 604.057, Axetris) is released from UV-dicing tape and printed on a Si wafer with alignment marks. The microstructure and alignment accuracy of these lenses are observed using VHX2000 Keyence 3D-Microscope and surface roughness is measured with a Bruker atomic force microscope (AFM) before and after printing.

2.1 Device Fabrication and Release

Double-sided polished 300 μm thick Si and 500 μm thick FS wafers were placed on UV-curable dicing tape and diced into Si (360×1000 μm^2) and fused-silica glass (815×2315 μm^2) pieces using a Disco DAD 2H/6T dicer with cutting speed of 5 mm/s and spindle speed of 30,000 rpm. These devices were released by exposing the back side of the wafer/tape with 250 mJ/cm^2 dose of UV at an exposure density of 10 mW/cm^2 using a SUSS Microtec MA6 mask aligner. The step-by-step process of releasing and transferring devices is shown in Fig. 2. To demonstrate printing of actual Si and FS lenses, 10$\times$ off-the-shelf lenses of each type supplied from Axetris (Part No. FCA250Si, silicon, 1×4 array, 250 μm array pitch, 240 μm lens diameter;

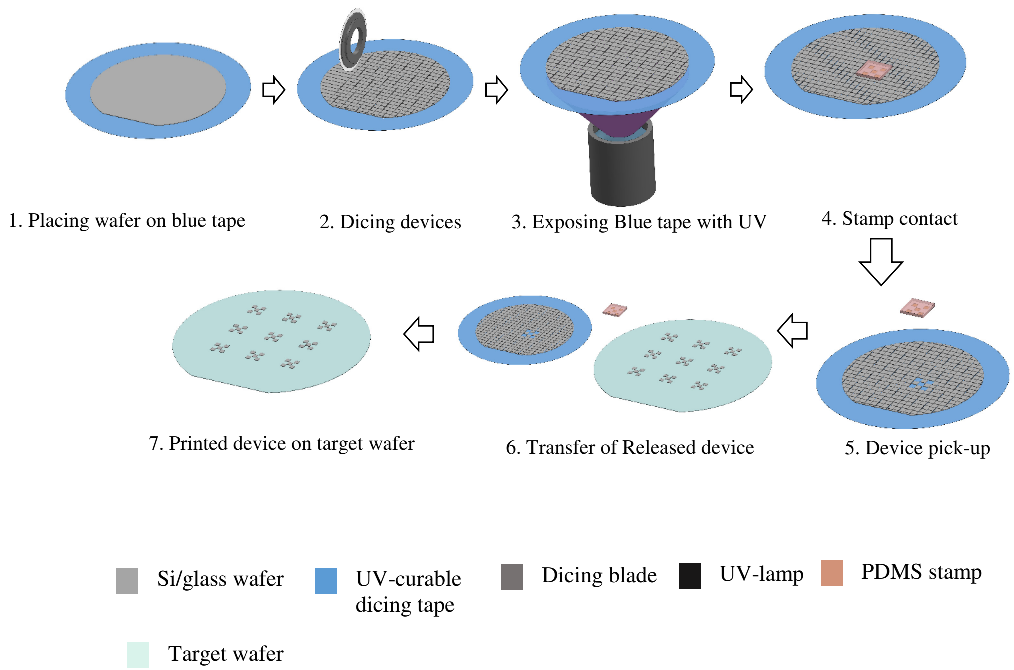

Fig. 2 Schematic of step-by-step μTP process using UV-release method.

Part No. FCA250FS, 1×8 array, 250 μm array pitch, and 240 μm lens diameter) are used.[38,39] These lenses are placed on UV-curable dicing tape with 6-in. dicing frame.

Silicon and fused-silica coupons of various sizes and thicknesses (300 to 1000 μm) are printed on a 4-in. silicon target wafer coated with 2 μm InterVia as shown in Fig. 3.

2.2 Device Printing

The PDMS stamp post area is critical to pick up these devices, post as small as 70% of coupon size are used to successfully pick-up and print device as printing depends on the contact area between two.[9] This is further discussed in Sec. 3.5. Three single-side polished Si wafers (2 with alignment marks and 1 without) are coated with 2 μm thick InterVia (adhesive) to be used as target wafers. InterVia is spin coated followed by 5 min of baking at 90°C. After this process is complete, the InterVia is exposed to UV light for 2 min, then baked for a further 3 min at 100°C. Next, the InterVia is hard-cured in an oven for 3 h at 175°C. As a result of curing, the InterVia bond becomes stronger, and the devices are seen to adhere strongly to the new target.

2.3 Shear Test

10 samples of the pseudo-Si and FS micro-lens arrays are used for shear testing analysis. This test is performed before and after InterVia curing using a Royce shear tester model 552 as per MIL-STD-883 standard. For normalization, shear strength is calculated in megapascal (MPa) to take into account different contact surface areas between different lenses. For comparison of strength, four samples of 4×4 mm^2 FS dies were bonded to a silicon substrate via a 2 μm thick layer of UV-curable Dymax-OP29 epoxy. A UV lamp was then used for 2 min to completely cure the epoxy. The shear strength of the bonded sample using InterVia was compared with Dymax-OP29 and optical epoxies used in the existing literature.

2.4 Microstructure of Bonded Pseudo Lenses

Two micro-transfer printed (Si on target Si wafer and FS on target Si wafer) and two epoxy bonded pseudo lenses are molded in epoxy to hardener ratio of 2:15 and kept for 8 h to get hard mold. The grinding of these molded samples is done from silicon carbide (SiC) abrasive papers of 400, 600, 800, 1200, 2500, and 3000 grits. Next, the polishing of these samples is done on SiC polishing cloth with 1 μm alumina suspension. To check the uniformity of the bonding

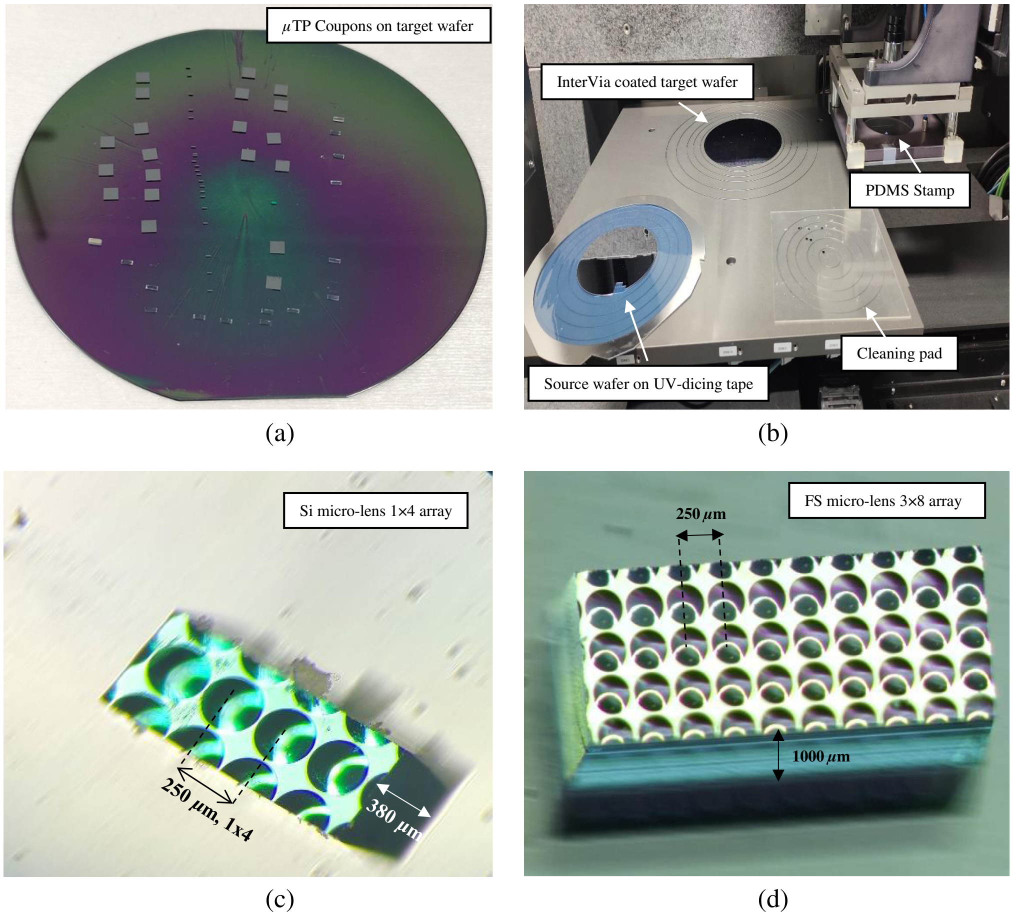

Fig. 3 (a) Image of Si and FS coupons printed on 2 μm thick InterVia coated target wafer, (b) X-celeprint machine set-up and (c), (d) higher magnified images showing printed Si and FS micro-lenses.

layer, SEM images of the left, center, and right corners of the polished sample are taken by FEI Quanta 650 SEM. Also, the thickness of InterVia is measured.

2.5 Microstructure and Alignment Accuracy of Actual Lenses

The microstructure of 20 lenses before and after printing is observed using VHX2000 Keyence 3D-Microscope at 500× and 1000× magnification. Horizontal and vertical misalignments and respective rotations are measured by printing 1000 μm thick lenses on the grating coupler (GC) of a PIC. Manually at higher magnification, the center of micro-lens was recognized during the pattern registration process, and this registration was kept the same for subsequent printing. After printing, the measurement of misalignment was captured by measuring the distance from the edge of the micro-lens to the alignment mark reference defined on the target and comparing them with designed distances without micro-lens.

2.6 Surface Roughness

The change in surface roughness of five lenses before and after μTP is determined using Bruker AFM. The test is performed by scanning $1 \times 1\ \mu\text{m}^2$ area of the lens top curve surface. The calculation of root mean square roughness (Sq) and leveling is done in Gwyddion software.

3 Results and Discussion

3.1 Shear Strength

The average shear strength of μTP $360 \times 1000\ \mu\text{m}^2$ pseudo-Si and $815 \times 2315\ \mu\text{m}^2$ FS lenses before and after InterVia curing is shown in Fig. 4.

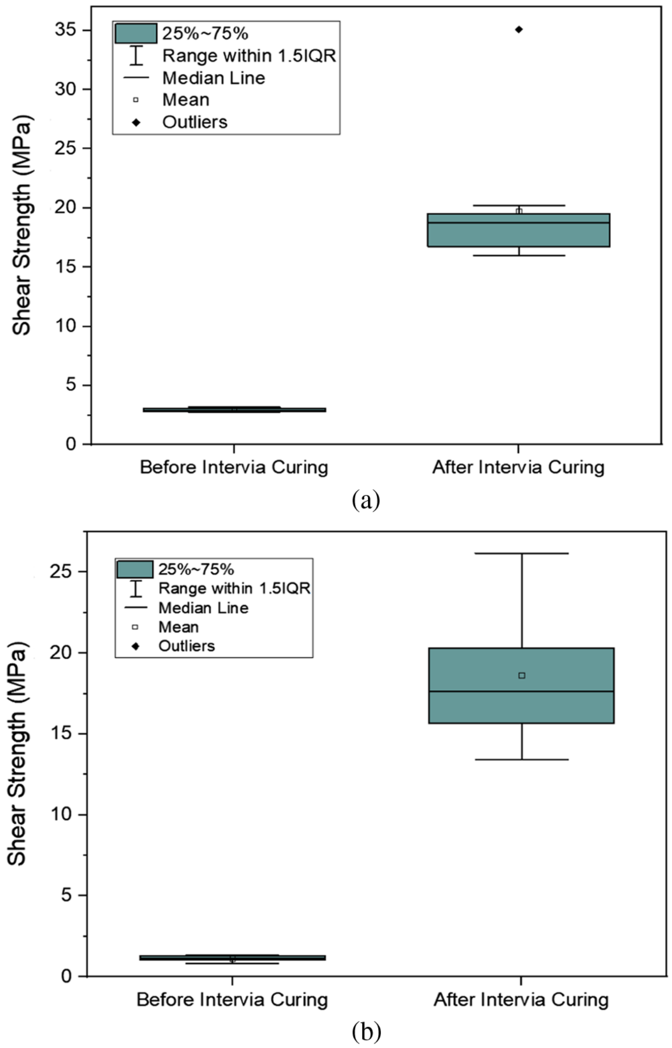

Fig. 4 Shear strength plots for (a) $360 \times 1000\ \mu\text{m}^2$ pseudo-Si micro-lens array and (b) $815 \times 2315\ \mu\text{m}^2$ pseudo FS micro-lens array.

After InterVia curing, the average shear strength of printed pseudo-Si lenses is 19.76 ± 5.5 MPa which is $\sim 10\times$ average shear strength before curing (2.9 ± 0.14 MPa). In the case of pseudo-FS lenses, after curing the average strength is 18.86 ± 4.9 MPa which is $\sim 10\times$ shear strength obtained before curing. Shear strength values obtained from pseudo-Si and FS lenses in the current study are compared with existing optical epoxies (Table 2).

As presented in Table 2, the shear strength of pseudo-Si lenses printed using InterVia is higher than most of the epoxies and comparable to Boble LV740 adhesive and BCB used in other studies. A comparison was also done between OP-29 Dymax optical epoxy and μTP samples using InterVia. The results in Table 2 demonstrate that the shear strength of micro-transfer printed Si on target Si (19.76 MPa) and FS on target Si (18.86 MPa) using InterVia is higher than FS on Si (6.84 MPa) prepared by optical epoxy OP-29. This makes InterVia a highly strong bonding material as compared to OP-29 epoxy.

3.2 Microstructure of Bonded Samples

SEM images of μTP Si on a Si target substrate are presented in Fig. 4. Pseudo-Si lenses are successfully bonded on the Si target substrate with no delamination observed at the Si-InterVia-Si interfaces [Fig. 5(a)]. The average thickness of InterVia is $2.54 \pm 0.03\ \mu$m. Similarly, pseudo-FS lenses are successfully printed on a target Si substrate with no delamination observed at FS-InterVia-Si interfaces [Fig. 5(b)]. The thickness of InterVia is $2.04 \pm 0.03\ \mu$m. Differences in thicknesses of Si-InterVia-Si and FS-InterVia-Si interfaces are due to thickness

Table 2 Comparison of shear strength of InterVia with existing studies.

Type of bonding materials	Shear strength (MPa)	References
Optical epoxy (R.I.: 1.56 at 1550 nm)	8.2	40
Boble LV740 UV adhesive	17	41
Epotek 377 non-UV	10	42
Epotek 353 Nd	>13.8	43
BCB	8.2 to 17	44
BCB <50 nm	2	45
UV epoxy resin	14.70	46
OP-29 Dymax (FS on Si)	6.84 ± 0.57	[This study]
InterVia (Si on Si)	19.76 ± 5.51	[This study]
InterVia (FS on Si)	18.86 ± 4.9	[This study]

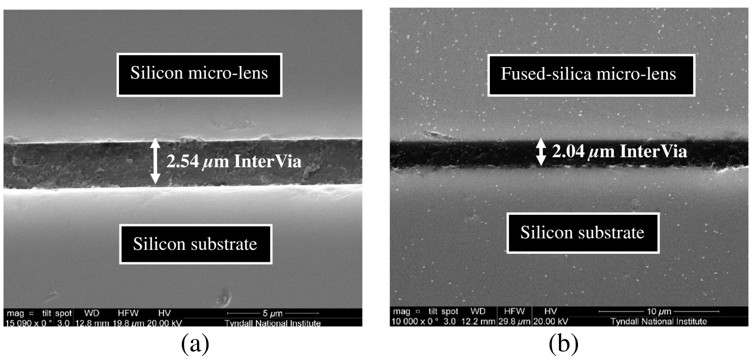

Fig. 5 SEM images of (a) silicon and (b) fused-silica micro-lenses μTP on silicon wafer showing InterVia on interface.

and area of coupon. For example, the thickness and area of Si coupons were 300 μm and 360×1000 μm^2 whereas the thickness and area of fused-silica coupons were 500 μm and 815×2315 μm^2, respectively. This could lead to different pressure distributions during the μTP process resulting in differences in thicknesses. InterVia is uniformly spread throughout the device with a thickness variation between the left, center, and right ends of 30 to 40 nm.

SEM images of the FS die bonded on Si substrate using Dymax epoxy are shown in Fig. 6. No delamination was found between the silicon-epoxy-glass interface and the gap between chips was 0.960 ± 0.040 μm.

3.3 Microstructure and Alignment Accuracy

The microstructure of the micro-lens arrays before and after printing is presented in Fig. 7. The surface of each lens in an array was analyzed. The diameter and height of lens, and pitch remained same after printing as of before printing. Also, no imprint or mark of stamp post and foreign particles on top surface of a lens was found. Therefore, the PDMS stamp contact with the top surface of the lens array during pick-up and printing did not change the surface and shape of the micro-lenses.

The horizontal and vertical misalignments of the center of the five micro-lenses array with respect to the origin considered on the target wafer are shown in Fig. 8.

The horizontal distance of the lens origin to origin in the target area (based on GDS design) was 542.9 μm whereas the measured distance after printing was 543.2 μm; therefore, the horizontal misalignment was 300 nm. Similarly, the expected vertical distance was 176.2 μm; however, the actual distance obtained after the printing process was 174.9 μm which was off by

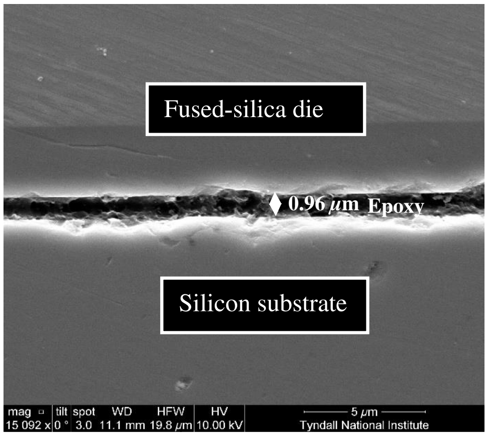

Fig. 6 SEM image of conventionally bonded dummy fused-silica die on silicon substrate showing 0.96 μm thick epoxy.

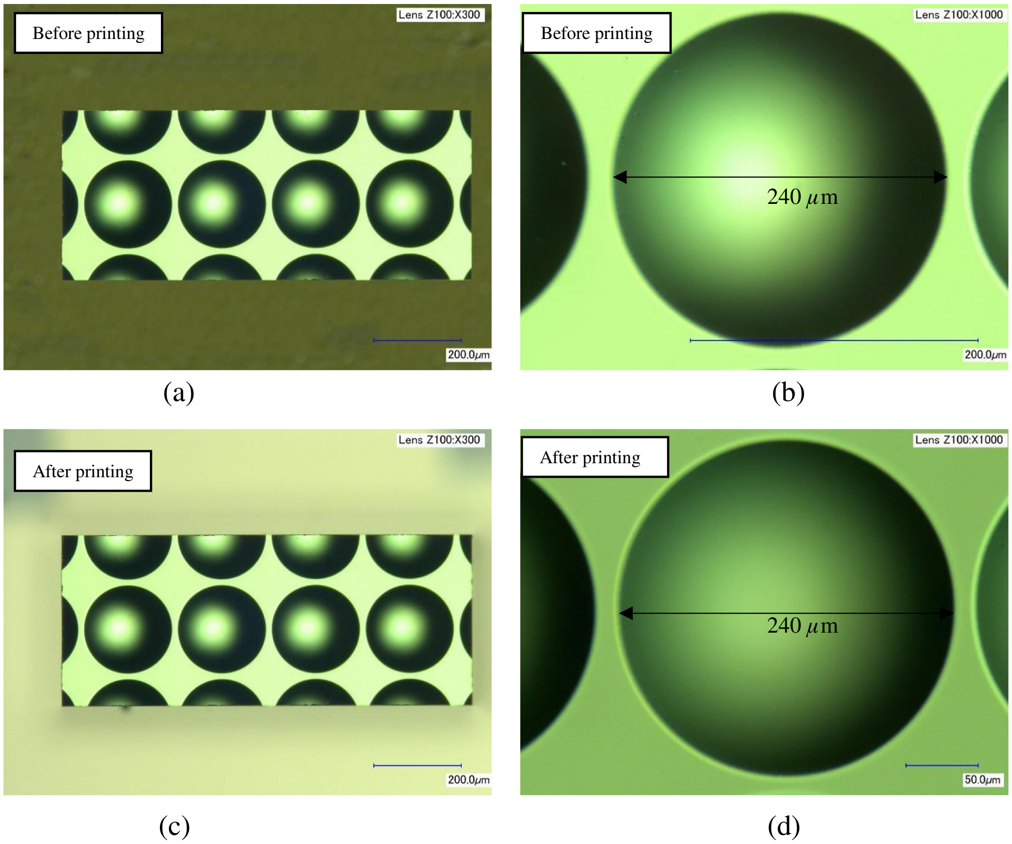

Fig. 7 3D-microscopic images of (a) 380 μm thick micro-lens array before printing, (b) single micro-lens before printing at higher magnification, (c) micro-lens array after printing, and (d) single micro-lens after printing at higher magnification.

1.3 μm. Rotational misalignments in horizontal and vertical directions were 0.0028 and 0.0024 deg, respectively (Table 3).

Alignment accuracy is very important for efficient optical coupling in photonic packaging as a few microns of misalignment result in a huge coupling loss.[38]

3.4 Surface Roughness

Sq value of the top curve surface of micro-lenses before and after printing was measured and AFM images of 1×1 μm^2 surface area are shown in Fig. 9.

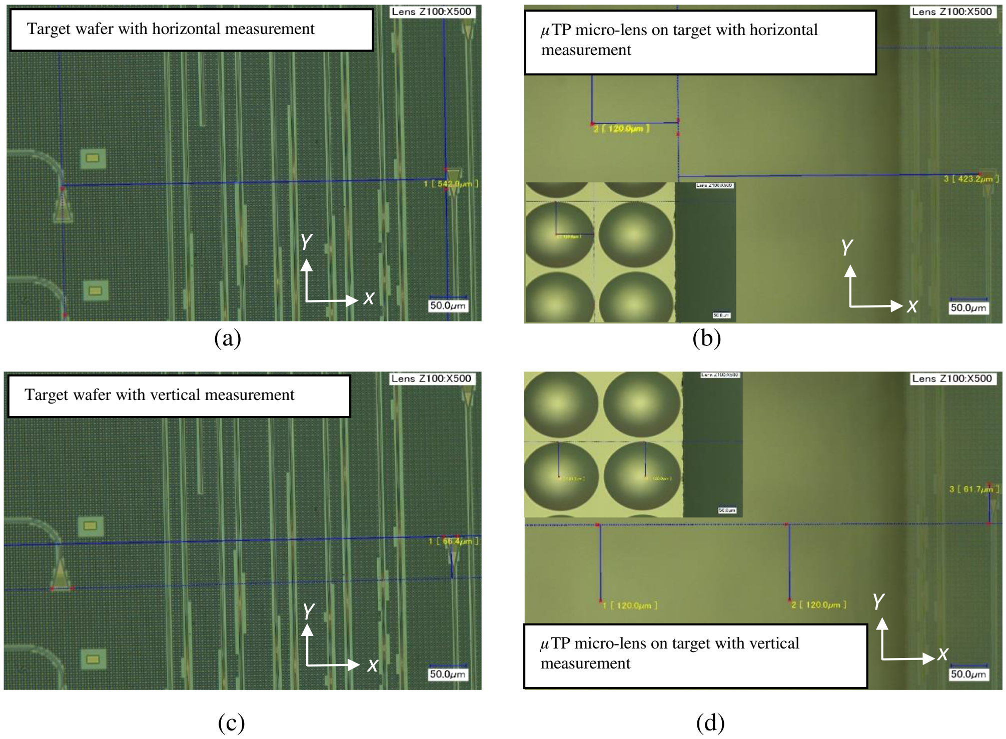

Fig. 8 Microscopic measurement of alignment area on (a), (c) target and (b), (d) micro-lens array printed on target.

Table 3 Misalignment calculation of μTP micro-lenses on grating coupler.

Before printing		After printing	
Center of GC to alignment mark on target (μm)		Center of lens to alignment mark on target (μm)	
X	Y	X	Y
−542.9	−176.2	−543.2	−174.9

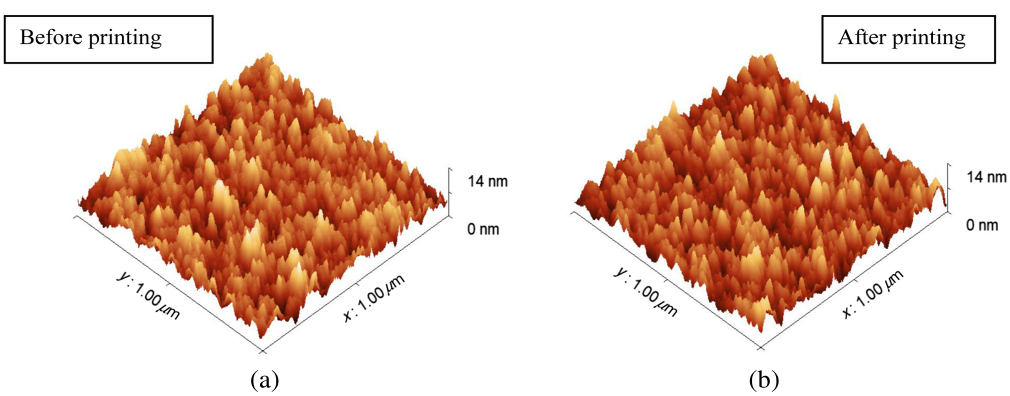

Fig. 9 AFM images of lens surface (a) before printing and (b) after printing.

The average values of Sq for five samples before and after printing were 1.750 ± 0.019 nm and 1.688 ± 0.025 nm. This shows that surface roughness of micro-lenses is not affected by (a) stamp post during pick-up and printing and (b) process parameters.

3.5 Discussion

This work presents the proof of concept for μTP thick optical components, especially lenses. These lenses can be used to expand and collimate the light beam, which can increase light coupling alignment tolerances significantly. μTP of optical components in photonics packaging will enable wafer-scale integration with high alignment accuracy. The higher shear strength of printed samples using InterVia could be related to the constituents involved in the preparation of polymer InterVia. Optical epoxies and InterVia are made of solvent, epoxy resin, coupling agent, and adhesives.[47–50] Based on the datasheet provided by suppliers, bisphenol A-(epichlorohydrin) epoxy resin (number average molecular weight ≤ 700) was used in InterVia.[48] Whereas OP-29 Dymax was prepared with 2-hydroxyethyl methacrylate (molecular weight $= 130$ g/mol) epoxy resin.[49] The strength of a polymer depends on its molecular weight, cross-linking, and crystallinity. Increasing the molecular weight enables more cross-linking/binding sites thereby giving higher strength to a polymer.[47] The higher molecular weight of epoxy resin used in InterVia can be the reason behind the higher shear strength of μTP samples using InterVia as compared to OP-29 optical epoxy bonded samples. InterVia thickness is a critical parameter, and it is seen that Si coupons as thick as 300 μm can be successfully printed on as thin as 50 nm InterVia layer. The average shear strength of 10 such printed coupons after curing was 5.85 ± 2.1 MPa. The microstructure of printed Si on Si target wafer is shown in Fig. 10.

Beyond 300 μm thickness of coupons, printing was not happening on 50 nm InterVia as coupons were shearing on target, but they did not leave stamp post as adhesion of coupons with stamp post was higher than 50 nm InterVia coated target wafer.[1,9] Failure to print on 50 nm thick InterVia could also be possibly due to the rougher back surface of that particular lot of coupons. Coupons with a thickness range of 300 to 1000 μm can be printed on ≥ 2 μm thick InterVia. After curing, the spin coating process gave the desired InterVia thickness of between 2 and 2.5 μm where the expected thickness before curing was 2 μm as shown in Figs. 4 and 5. In the conventional way of die bonding using epoxy dispensing processes, the expected thickness was 2 μm; however, the realized thickness measured afterward was 0.9 to 1 μm (Fig. 6). Due to challenges in the conventional way of die bonding process, the epoxy thickness was difficult to control. Whereas InterVia thickness due to the spin coating process was controlled to a few nanometers. This shows that spin coating and μTP processes are more stable and uniform than conventional die bonding and epoxy dispensing techniques.

It is important to discuss stamp post area selection for picking up thick optical components as stamp post area optimization is critical. From various experiments on different coupon sizes (460×1100 μm^2, 360×1000 μm^2, 815×2315 μm^2, 3000×3000 μm^2, 700×4000 μm^2,

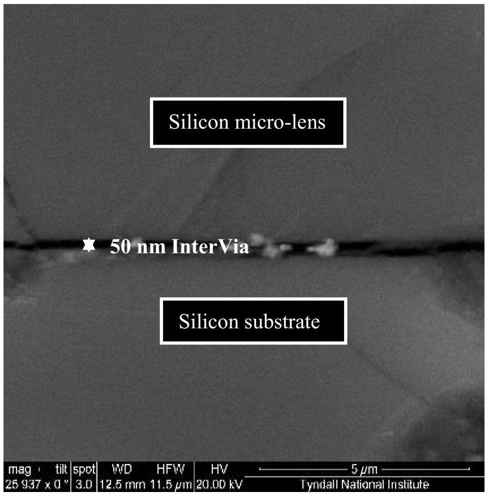

Fig. 10 SEM image of Si μTP on 50 nm InterVia coated Si target.

$800 \times 3000\ \mu m^2$, $800 \times 1500\ \mu m^2$), it is found that area of stamp post should be in the range of 30% to 70% of coupon area. For 2 μm thick InterVia, stamp posts smaller than 30% were not able to pick up coupons whereas stamp post areas higher than 70% were decreasing print yield as the pick-up and printing process rely on the contact area between coupon and stamp.[1,9] In summary, the post area ~70% of the coupon area is most desirable for printing with high yield.

In the μTP process, a PDMS stamp is put in contact with the lens surface and process parameters, such as shear distance, speed, and retraction, may change the microstructure and roughness of lenses. This change in roughness will affect the coupling of light in and out of the PIC.[50] The highly rough surface of optical devices reduces light coupling due to scattering.[51–53] This has been proven in a study where the effect of surface roughness of fiber surface on light coupling efficiency was demonstrated.[53] The results showed the amount of light coupled increased by double when average surface roughness declined from 45 to 2 nm. In our study, the surface roughness of the micro-lens array is within the specs provided by the supplier.[39] Also, the μTP process did not introduce any additional roughness.

4 Conclusion and Future Study

This study presented the proof of concept for μTP of thick optical components for the first time. Based on the results obtained, the following conclusions can be made:

- Optical components, such as lenses and prisms in 250 to 1000 μm thickness range, can be successfully micro-transfer printed on silicon target wafers. This will enable wafer-scale assembly of optical components in photonic packaging.
- Cured InterVia has higher bond strength (19 MPa) than widely used UV-curable optical epoxies (2 to 17 MPa). This shows that InterVia could be a good bonding material.
- InterVia is uniformly coated throughout the target wafer as shown by SEM images. Its thickness is well-controlled and uniform.
- It is also proven that PDMS stamp contact to lenses and pick-up and print process parameters, such as overdrive distance, shear distance, shear speed, do not affect microstructure and surface roughness of lenses.

Future work will investigate the effect of different thicknesses of InterVia on printing yield and shear strength. Printing of thick lenses on glass wafers can also be demonstrated. Most importantly, a surface-assembled demonstrator can be built by μTP lenses on grating and edge couplers to demonstrate the application of this technique in a real-world optical system.

Code and Data Availability

All data in support of the findings of this paper are available within the article.

Acknowledgments

This work was supported by PIADS and Science Foundation Ireland (SFI) through the Irish Photonic Integration Centre (IPIC) under 18/EPSRC-CDT/3585. The authors would like to thank Sean Collins for his help with mechanical design and Dan O'Connell for his help with the UV curing of wafers.

References

1. B. Corbett, et al., "Transfer printing for silicon photonics," in *Semiconductors and Semimetals*, S. Lourdudoss, R. T. Chen, and C. Jagadish, Eds., Vol. **99**, pp. 43–70, Elsevier (2018).
2. J. Zhang et al., "Integrated optical transmitter with micro-transfer-printed widely tunable III-V-on-Si laser," in *Opt. Fiber Commun. Conf.*, Optica Publishing Group (2022).
3. J. Zhang et al., "Silicon photonics fiber-to-the-home transceiver array based on transfer-printing-based integration of III-V photodetectors," *Opt. Express* **25**(13), 14290–14299 (2017).
4. G. Roelkens et al., "Transfer printing for silicon photonics transceivers and interposers," in *IEEE Opt. Interconnects Conf.*, IEEE (2018).
5. K. Rae et al., "Transfer-printed micro-LED and polymer-based transceiver for visible light communications," *Opt. Express* **26**(24), 31474–31483 (2018).

6. X. Zhou et al., "Growth, transfer printing and colour conversion techniques towards full-colour micro-LED display," *Prog. Quantum Electron.* **71**, 100263 (2020).
7. Z. Shaban, "Micro-transfer printing of micro-structured, ultra-thin light-emitting devices," https://hdl.handle.net/10468/14474 (2023).
8. J. Zhang et al., "III-V-on-silicon widely tunable laser realized using micro-transfer-printing," in *45th Eur. Conf. Opt. Commun.*, IET (2019).
9. B. Haq, "III-V-on-Si SOAs and DFB/DBR lasers realised using micro-transfer printing," Doctoral dissertation, Ghent University (2021).
10. J. Goyvaerts et al., "Enabling VCSEL-on-silicon nitride photonic integrated circuits with micro-transfer-printing," *Optica* **8**(12), 1573–1580 (2021).
11. G. Roelkens, J. Bauwelinck, and J. Campenhout, "III-V-on-silicon photonic transceivers," in *IEEE Photonics Conf. (IPC)*, IEEE (2019).
12. G. Chen et al., "Integration of high-speed GaAs metal-semiconductor-metal photodetectors by means of transfer printing for 850 nm wavelength photonic interposers," *Opt. Express* **26**(5), 6351–6359 (2018).
13. J. Justice et al., "Wafer-scale integration of group III–V lasers on silicon using transfer printing of epitaxial layers," *Nat. Photonics* **6**(9), 610–614 (2012).
14. J. Zhang et al., "Transfer-printing-based integration of a III-V-on-silicon distributed feedback laser," *Opt. Express* **26**(7), 8821–8830 (2018).
15. R. Loi et al., "Transfer printing of AlGaInAs/InP etched facet lasers to Si substrates," *IEEE Photonics J.* **8**(6), 1504810 (2016).
16. R. Loi et al., "Thermal analysis of InP lasers transfer printed to silicon photonics substrates," *J. Lightwave Technol.* **36**(24), 5935–5941 (2018).
17. G. Muliuk et al., "Transfer print integration of 40Gbps germanium photodiodes onto silicon photonic ICs," in *Eur. Conf. Opt. Commun. (ECOC)*, IEEE (2017).
18. T. Vanackere et al., "Micro-transfer printing of lithium niobate on silicon nitride," in *Eur. Conf. on Opt. Commun. (ECOC)*, IEEE (2020).
19. T. Meissner et al., "High speed etched facet traveling wave modulators for micro transfer print integration," in *CLEO: Appl. and Technol.*, Optica Publishing Group (2022).
20. Z. Li et al., "Photonic integration of lithium niobate micro-ring resonators onto silicon nitride waveguide chips by transfer-printing," *Opt. Mater. Express* **12**(11), 4375–4383 (2022).
21. T. Vandekerckhove et al., "Reliable micro-transfer printing method for heterogeneous integration of lithium niobate and semiconductor thin films," *Opt. Mater. Express* **13**(7), 1984–1993 (2023).
22. R. Lerner et al., "Integration of GaN HEMTs onto silicon CMOS by micro transfer printing," in *28th ISPSD*, IEEE (2016).
23. R. Lerner et al., "Heterogeneous integration of microscale gallium nitride transistors by micro-transfer-printing," in *IEEE 66th ECTC*, IEEE (2016).
24. D. A. Carter et al., "Si/InP heterogeneous integration techniques from the wafer-scale (hybrid wafer bonding) to the discrete transistor (micro-transfer printing)," in *IEEE S3S*, IEEE (2018).
25. R. Lerner et al., "Flexible and scalable heterogeneous integration of GaN HEMTs on Si-CMOS by micro-transfer-printing," *Phys. Status Solidi-a* **215**(8), 1700556 (2018).
26. J. D. Meyer et al., "Micro-transfer printing technology for GaN transistors," ECS 236. No. 25, The Electrochemical Society, Inc. (2019).
27. R. Reiner et al., "Characteristics of hetero-integrated GaN-HEMTs on CMOS technology by micro-transfer-printing," in *33rd Int. Symp. on Power Semicond. Devices and ICs (ISPSD)*, IEEE (2021).
28. P. B. Downey et al., "Micro-transfer printing of GaN HEMTs for heterogeneous integration and flexible RF circuit design," in *Device Res. Conf.*, IEEE (2020).
29. Z. Liu et al., "Micro-transfer printed silicon nitride grating couplers for efficient on-chip light coupling," *Proc. SPIE* **12004**, 1200404 (2022).
30. N. K. Wessling et al., "Fabrication and transfer printing-based integration of free-standing GaN membrane micro-lenses onto semiconductor chips," *Opt. Mater. Express* **12**(12), 4606–4618 (2022).
31. N. K. Wessling et al., "Integration of single GaN micro-lenses with high index semiconductors by transfer printing," in *CLEO: QELS_Fundam. Sci.*, Optica Publishing Group (2022).
32. C. Scarcella et al., "Pluggable single-mode fiber-array-to-PIC coupling using micro-lenses," *IEEE Photonics Technol. Lett.* **29**(22), 1943–1946 (2017).
33. K. Gradkowski et al., "Demonstration of a single-mode expanded-beam connectorized module for photonic integrated circuits," *J. Lightwave Technol.* **41**(11), 3470–3478 (2023).
34. "Mode field diameter and numerical aperture," (2020). https://www.thorlabs.com/newgrouppage9.cfm?objectgroup_id=14204.
35. B. Corbett et al., "Transfer print techniques for heterogeneous integration of photonic components," *Prog. Quantum Electron.* **52**, 1–17 (2017).

36. K. Oswalt et al., "Micro transfer printing various thickness components directly from dicing tape," in *IEEE 73rd Electron. Components and Technol. Conf. (ECTC)*, IEEE (2023).
37. S. Pal et al., "A study on a tether-less approach towards micro-transfer-printing of large-footprint power micro-inductor chiplets," in *IEEE 3DIC*, IEEE (2023).
38. I.-V. Bundalo et al., "PIXAPP photonics packaging pilot line–development of a silicon photonic optical transceiver with pluggable fiber connectivity," *IEEE J. Sel. Top. Quantum Electron.* **28**(3), 8300311 (2022).
39. Axetris, "Microlens," https://www.axetris.com/en-cn/axetris/moe-and-services/products/refractive/fca-microlenses (accessed 31 August 2017).
40. A. Marinins et al., "Wafer-scale hybrid integration of InP DFB lasers on Si photonics by flip-chip bonding with sub-300 nm alignment precision," *IEEE J. Sel. Top. Quantum Electron.* **29**(3), 8200311 (2022).
41. Bohle, "UV-Klebstoff Verifix LV 740," 1–2 (n.d.). https://www.bohle.com/en-gb/products/glass-bonding/adhesives/2474/uv-adhesive-verifix-lv-740
42. Epoxy Technology, "EPO-TEK 353ND," 1–2 (2014). https://www.epotek.com/docs/en/Datasheet/353ND.pdf.
43. Epoxy Technology, "EPO-TEK 377," 1–2 (2015). https://www.epotek.com/docs/en/Datasheet/377.pdf.
44. W. Xia et al., "Benzo-cyclo-butene bonding process with 'stamp'printing for wafer level package," *Micro Nano Lett.* **9**(5), 363–366 (2014).
45. S. Keyvaninia et al., "Ultra-thin DVS-BCB adhesive bonding of III-V wafers, dies and multiple dies to a patterned silicon-on-insulator substrate," *Opt. Mater. Express* **4**(1), 35–46 (2013).
46. T. Matsumoto et al., "Hybrid-integration of SOA on silicon photonics platform based on flip-chip bonding," *J. Lightwave Technol.* **37**(2), 307–313 (2018).
47. Omnexus, "Plastic and elastomers," Tensile Strength - Definition, Units, Formula & Test Methods, specialchem.com
48. Kayakum, "InterVia photodielectric," https://kayakuam.com/wp-content/uploads/2019/09/Intervia-Photodielectric-8023-UL-PF08N013R2.pdf.
49. Dymax, "OP-29," https://dymax.com/products/formulations/light-curable-materials/bonding/dissimilar-substrate-bonding/op-29.
50. S. Wakeel et al., "Constituents and performance of no-clean flux for electronic solder," *Microelectron. Reliab.* **123**, 114177 (2021).
51. M. Zickar et al., "MEMS compatible micro-GRIN lenses for fiber to chip coupling of light," *Opt. Express* **14**(10), 4237–4249 (2006).
52. R. Kirchner et al., "How post-processing by selective thermal reflow can reduce the roughness of 3D lithography in micro-optical lenses," *Proc. SPIE* **10095**, 1009507 (2017).
53. A. Y. Gharbia, M. Gareth, and K. Jayantha, "The effect of optical fiber endface surface roughness on light coupling," *Proc. SPIE* **5252**, 201–208 (2004).

Biographies of the authors are not available.